# Non-dissipative anomalous currents in 2D materials: the parity magnetic effect as an analog of the chiral magnetic effect

Ana Júlia Mizher, 1, 2, \* David Dudal, 3, 4, † Filipe Matusalem, 5, ‡ Alexandre Reily Rocha, 2, § and Cristian Villavicencio  $^{1,6}$ , ¶

Anomalous electric currents along a magnetic field, first predicted to emerge during large heavy ion collision experiments, were also observed a few years ago in condensed matter environments, exploring the fact that charge carriers in Dirac/Weyl semi-metals exhibit a relativistic-like behavior. The mechanism through which such currents are generated relies on an imbalance in the chirality of systems immersed in a magnetic background, leading to the so-called *chiral magnetic effect* (CME). While chiral magnetic currents have been observed in materials in three space dimensions, in this work we propose that an analog of the chiral magnetic effect can be constructed in two space dimensions, corresponding to a novel type of intrinsic half-integer Quantum Hall effect, thereby also offering a topological protection mechanism for the current. While the 3D chiral anomaly underpins the CME, its 2D cousin is emerging from the 2D parity anomaly, we thence call it the *parity magnetic effect* (PME). It can occur in disturbed honeycomb lattices where both spin degeneracy and time reversal symmetry are broken. These configurations harbor two distinct gap-opening mechanisms that, when occurring simultaneously, drive slightly different gaps in each valley, establishing an analog of the necessary chiral imbalance. Some examples of promising material setups that fulfill the prerequisites of our proposal are also listed.

# I. INTRODUCTION

The chiral magnetic effect (CME) is an anomalous electric current generated from an imbalance in the chirality of massless fermions in three spatial dimensions in the direction of an external magnetic field. It was first proposed to possibly occur in the quark-gluon plasma created in heavy-ion collisions. The physical principle behind the CME crucially depends on a very intense magnetic field intrinsically present in non-central collisions [1, 2]. The chiral imbalance is induced by the mediators of the strong force—the gluons—as these gauge particles can support a field configuration with a non-trivial topology. The interaction of the fermions with topological gluons, as facilitated by the chiral anomaly, triggers a mechanism that generates a polarization in the final state that could be observed in the detectors. This current is represented in Fig. 1(a).

When dealing with the quark-gluon plasma, the current usually is written in terms of an effective chiral chemical potential,  $\mu_5$ , without scrutinizing the details of the utterly complicated interaction between topological gluons and quarks,

$$\vec{J}_{\text{CME}} = \frac{e^2}{2\pi^2} \mu_5 \vec{B}. \tag{1}$$

This expression does not depend on how the imbalance was created, as long as it is present. Although there is some evidence for the CME happening in the quark-gluon plasma the issue of disentangling the possible signal from other sources [3] is still unresolved [4].

Recently discovered Weyl and Dirac semi-metals have opened such a new avenue that, among a plethora of applications, allows for connections between high energy phenomena and condensed matter physics due to the linear

<sup>\*</sup> ana.mizher@unesp.br

<sup>†</sup> david.dudal@kuleuven.be

 $<sup>^{\</sup>ddagger}$ fmatusa@unicamp.br

<sup>§</sup> alexandre.reily@unesp.br

 $<sup>\</sup>P$  cvillavicencio@ubiobio.cl

dispersion in these materials, a feature that is typically associated to relativistic particles [5]. Exactly due to this relativistic-like behavior, combined with the low energies associated, it is possible to construct table top setups to explore certain phenomena proposed to happen in particle physics but that are too hard to observe due to the complexity of the experimental apparatus and data analysis in this field. Remarkable examples are the Klein paradox [6] and the Zitterbewegung [7].

Based on this, the fast-growing family of discovered Weyl-Dirac materials have allowed to test a simpler version of the CME in a condensed matter environment, with explicit experimental verification in several three-dimensional Dirac materials [8, 12–17]. In this framework, the chiral anomaly is generated by co-linear electric and magnetic fields [18], which induces an anomalous electric current in the field direction. Remarkably, this current is symmetric under time reversal transformation, which means it is dissipation-less. Due to this feature, it is believed that materials that support the CME could replace superconductors in certain devices, with the extraordinary advantage that it performs at higher temperature. A significant advantage of the condensed matter CME compared to its high energy counterpart is that in the former case, the chiral chemical potential is tunable.

Unfortunately, it has the drawback that the chirality scatters in time since in Dirac semi-metals the left- and right-handed fermions can mix [8].

At the same time, two-dimensional materials such as graphene [9] and transition metal dichalcogenides form a new family of materials from both the fundamental aspects as well applications [10, 11]. The situation for a possible effect resembling that of the CME in two dimensions, however, is somewhat more complicated. A low energy tight binding description of planar Dirac materials arranged in a honeycomb lattice yields a Clifford algebra associated to the sublattice, or pseudo-spin degree of freedom [19, 20]. Despite that in two dimensions it is not possible to define the chiral operator  $\gamma_5$ , it is possible to combine the spinors associated to each Dirac point in a four-component spinor containing sublattice and valley degrees of freedom. This corresponds to a merging of the two representations in a new, reducible, four-component one [21]. In this fashion, the usual  $4 \times 4$  Dirac matrices emerge [19] and it is possible to define an operator analogous to the (3+1)-dimensional chirality operator  $\gamma_5$  which commutes with the Hamiltonian, indicating a conserved quantum number. The eigenstates from the Hamiltonian,  $\psi_k$  and  $\psi_{k'}$ , are eigenstates of this operator with eigenvalues  $\pm 1$ . Therefore, in terms of group theory, the valley degree of freedom corresponds to pseudo-chirality.

Although the pseudo-spin and pseudo-chirality share exactly the same group theory with the spin and chirality respectively, this correspondence has mostly been considered as a mere analog. Nevertheless it was shown that the situation may drastically change when the sublattice symmetry is broken and consequently a gap is opened [23, 24]. In this case, experimental observations indicate there is an angular momentum associated with the pseudo-spin, giving it a remarkable physical meaning.

# II. PME IN 2D: THEORETICAL SETUP AND NON-ZERO CONDUCTIVITY

Since there is no room for a chiral anomaly in 2D, one might deem currents à la CME impossible. However, there is room for a parity anomaly in 2D [25, 26], and here we will precisely exploit this anomaly to introduce the parity magnetic effect in 2D, which very much alike the 3D CME is characterized by a magnetic field driven current, which is non-dissipative.

We explore a honeycomb lattice with broken sublattice symmetry, as represented in Fig. 1(b). It has been shown that the difference in the energy of the electrons belonging to different sublattices can be parameterized at the Hamiltonian level via an effective standard fermion mass for two two-component spinors,  $\pm m$ , with opposite sign for each valley [26]. This induces a gap opening that preserves time reversal symmetry. In this case both valleys present symmetric gaps as represented in Fig. 1(c). It is also known that the anomalous T-odd piece of the electric current generated by an external field acting on this system is related to a topological Chern-Simons term [27]. In other words, it depends solely on the sign of the mass term and not on its magnitude. In presence of an external gauge field in two spatial dimensions, one gets

$$j^{i}(x) = \frac{e^{2}}{4\pi} \frac{m}{|m|} \epsilon^{ijk} F_{jk}(x) = \frac{e^{2}}{4\pi} \operatorname{sign}(m) \epsilon^{ijk} F_{jk}(x), \tag{2}$$

indicating that the net current vanishes when one sums up the contribution of both valleys [26].

In this work we add two new ingredients to the case previously considered. First of all, we allow for arbitrary values of the gaps associated to each Dirac point,  $m_k$  and  $m_{k'}$ , enabling configurations where  $m_k \neq m_{k'}$ . This corresponds to a band structure where the two valleys have asymmetric gaps, as represented in Fig. 1(d). Secondly, we include a chemical potential in order to explore certain regions of the band structure. The reason for this flexibility and how we calibrate the chemical potential will soon become clear.

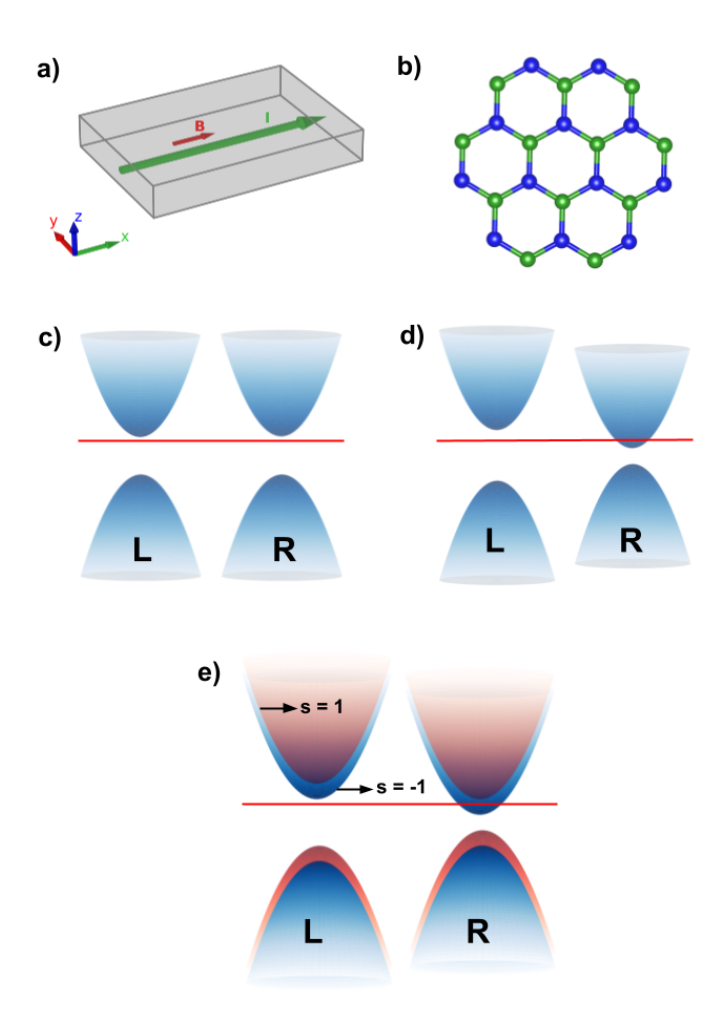


FIG. 1. (a) The parity magnetic effect generates an electric current along the external magnetic field; (b) Honeycomb lattice with broken sublattice symmetry; (c) Dirac cones with simple gap, analogous to the chirally symmetric case; (d) Valley asymmetry corresponding to imbalance in chirality; (e) Schematic representation of the band structure when a spin split is present besides valley asymmetry.

For pure honeycomb lattices composed by one type of atom per lattice site, such as pristine graphene, the Lagrangian obtained from the continuum limit of the tight-binding model is very similar (apart from the Fermi velocity breaking Lorentz invariance) to the fermion sector of Quantum Electrodynamics in two space and one time dimensions [19, 20],

$$\mathcal{L} = \sum_{s} \bar{\psi}_{s} \left( i \gamma^{0} \hbar \partial_{t} + i \hbar v_{F} \gamma^{x} D_{x} + i \hbar v_{F} \gamma^{y} D_{y} \right) \psi_{s}. \tag{3}$$

Here the index s labels the (electron) spin and the covariant derivative  $D_{\alpha} = \partial_{\alpha} + (ie/\hbar c)A_{\alpha}$ .  $A_{\alpha}$  is the gauge field associated to the electromagnetic interaction and the fields  $\psi_s \equiv \psi_s(t, \mathbf{r})$  denote four-component spinors that account for both valley and pseudospin index.

To make the valley degree of freedom more transparent we rewrite our Lagrangian using the pseudo-chiral projections. Decomposing the fermion field as

$$\psi = \psi_k + \psi_{k'} = \frac{1}{2} (1 + \gamma_5) \psi + \frac{1}{2} (1 - \gamma_5) \psi, \tag{4}$$

we can split the Lagrangian in Eq. (3) in two terms, associated to left and right pseudo-chiralities. We introduce untied gaps for each pseudo-chirality, allowing each projection to have different masses. The resulting Lagrangian is [29, 30]

$$\mathcal{L} = \sum_{s,\chi=k,k'} \bar{\psi}_{\chi,s} [i\gamma^0 \hbar \partial_t + \mu \gamma^0 + i\hbar v_F \gamma^x D_x + i\hbar v_F \gamma^y D_y + m_{s,\chi} \gamma^z] \psi_{\chi,s},$$

where we included the chemical potential,  $\mu$ , and a more general mass gap structure with  $m_{s,k}^2 \neq m_{s,k'}^2$ .

Within linear response theory the electric current we are interested in is defined as the product of a (parity) anomalous conductivity and a constant external magnetic field.

$$\langle \vec{j} \rangle = \sigma_{\chi} \vec{B}. \tag{5}$$

This formalism has been successfully applied to several transport phenomena in Dirac/Weyl materials [31, 32],

To extract the DC PME conductivity, we will benefit of some of the special properties of our mixed-dimensional system—the gauge fields are not restricted to a plane, while the fermions are—the proper framework to describe it being pseudo-QED [35, 36] or reduced-QED (RQED) [37].

We temporarily consider a time-varying magnetic field, and ultimately the limit  $\omega \to 0$  will yield the desired constant magnetic background field. The external (classical) magnetic field reads

$$\vec{B} = Be^{i\omega z}\cos(\omega t)\vec{e}_x,\tag{6}$$

in natural units where  $\hbar = c = 1$ . We can conveniently choose as vector potential

$$\vec{a} = \frac{i}{\omega} B \cos(\omega t) e^{i\omega z} \vec{e}_y, \tag{7}$$

which also comes with an electric field

$$\vec{E} = iBe^{i\omega z}\sin(\omega t)\vec{e}_{y}.$$
(8)

This set of external electromagnetic fields  $(\vec{E}, \vec{B})$  is physically acceptable as solving all Maxwell equations, for whatever value of  $\omega$ . For  $\omega \to 0$ , we find our desired field configuration,  $\vec{B} = B\vec{e}_x$ ,  $\vec{E} = 0$ . In Appendix A, we have scrutinized the Kubo relation to extract the DC PME conductivity, which upon using the crucial Eq. (B9) can be reexpressed as

$$\sigma_{\chi} = -\lim_{\omega \to 0} \frac{1}{\hbar \omega} \tilde{\Pi}_{R}^{xy},\tag{9}$$

where  $\tilde{\Pi}_R^{xy}$  is the xy-component of the RQED retarded (gauge invariant) polarization tensor. The PME depends solely on the T-odd contribution to this polarization tensor, i.e the piece proportional to the Levi-Civita tensor  $\epsilon^{ijk}$ . Similarly to what occurs in two-dimensional QED [32], the low frequency T-odd contribution is completely defined at one-loop order, that is, not receiving any higher order quantum corrections [38]. This is the Coleman-Hill theorem [39] generalized to RQED, resulting in a "topological" Chern-Simons mass term in the effective action. Moreover, that relevant contribution is also independent of the Fermi velocity  $v_F$  [38]. At one-loop the polarization tensor is only depending on fermion propagators, which are just the same as in usual planar QED.

Interestingly enough, the very same polarization tensor appears in the calculation of the (DC) Quantum Hall effect [40]. The difference is that we do not have an external electric field present, neither is the source of the anomalous conductivity a magnetic field orthogonal to the material's plane. Said otherwise, the possibility of the PME conductivity is intimately linked to that of an (intrinsic) anomalous Quantum Hall effect [41, 42], albeit leading to a current along a constant in-plane magnetic field rather than one orthogonal to an in-plane constant electric field. Performing the calculation of the T-odd piece of the polarization tensor and inserting it in Eq. (9) leads to

$$\sigma_{\chi} = \sum_{s} \frac{e^2}{4\pi} \left[ \frac{m_{s,k}}{|m_{s,k}|} \theta(m_{s,k}^2 - \mu^2) - \frac{m_{s,k'}}{|m_{s,k'}|} \theta(m_{s,k'}^2 - \mu^2) \right], \tag{10}$$

where  $m_{s,k}$  and  $m_{s,k'}$  are the gaps associated to each valley, per spin choice. Details can be found in Appendix B.

This is our main result. We note that for the configuration considered in previous works [24, 26], where  $|m_{s,k}| = |m_{s,k'}|$ , the net current vanishes as expected, but let us consider the case where the gaps differ, represented in Fig. 1(d). Then the system does enjoy neither an inversion center nor time reversal invariance, implying an uplifting of the pseudo-chiral fermions degeneracy. The most immediate way to achieve such a configuration is to work simultaneously with a double gap opening mechanism. On top of the inversion symmetry breaking mass term,  $\delta \tau_z \otimes \sigma_z$ —with  $\tau$  designating the valley whilst  $\sigma$  relating to sublattice—discussed previously [26], we propose to add an interaction capable of inducing a time reversal symmetry breaking. This corresponds to a mass term where the sign of the masses remain the same in both valleys,  $\Delta \tau_0 \otimes \sigma_z$ . A configuration subject to both symmetry breaking mechanisms will lead to different gaps in each valley as required.

The coupling of the masses to spin must be chosen carefully, otherwise currents associated to different spins cancel each other. First of all, we require that a spin flip causes a global change of sign, not a relative one. This is crucial

otherwise for each spin a different valley will be favored, inflicting a cancellation. That is the reason a Kane-Mele type of configuration [44] does not satisfy our conditions. In order to avoid this situation we choose to add the following mass couplings

$$m_{s,k}\sigma_z = s(\Delta + \delta)\sigma_z, \qquad m_{s,k'}\sigma_z = s(\Delta - \delta)\sigma_z.$$

to the Lagrangian, with  $\Delta > \delta$ .

Notice however that a flip in spin induces a flip in mass sign. We can check from Eq. (10) that this also would induce a cancellation between currents belonging to the same valley with different spin. We will consider this observation below, when we seek for suitable materials that fulfill our conditions.

Synthesizing the discussion above, a planar material capable to support the CME must (i) contain Dirac points (ii) present inversion symmetry breaking (iii) present time reversal symmetry breaking and (iv) present a split in spin bands.

If these conditions are met, we thus predict from Eq. (10) a DC CME current given by

$$\vec{j} = \sigma_{\chi} \vec{B}, \qquad \sigma_{\chi} = \frac{c}{2} \frac{e^2}{h}.$$
 (11)

where we reintroduced the units, including the prefactor c related to having a current along a magnetic rather than electric field.

As we explained before, this anomalous conductivity will receive no further quantum corrections, which is suggestive of a topological protection mechanism. That this is indeed the case is scrutinized in the Appendix C, where we lay the connection with a half-integer anomalous Quantum Hall effect in detail, not unlike the situation of the magnetically doped (BiSb)<sub>2</sub>(TeSe)<sub>2</sub> materials reviewed in [41] albeit that the underlying mechanism is quite different in our case. Indeed, we are *not* looking at the single Dirac cone per surface of a three-dimensional topological insulator, rather our judicious choice of model parameters in our genuine two-dimensional material eliminates one of the two cones from the game. Moreover, we do not have to rely on band inversion. What is common in both situations is that the effective low energy dynamics around the relevant Dirac point is attributable to a continuum Chern-Simons term, radiatively generated by the massive fermions.

# III. PME IN 2D: PROMISING MATERIALS

A few candidates present the features that meet these criteria, as calculated using *ab initio* methods. In general, monolayer crystals with high potential to be applied in valleytronics physics are good candidates. First of all, manganese chalcogenophosphate MnPSe<sub>3</sub> is organized in honeycomb lattices and it is intrinsically gapped. The material counts on two mechanisms to open the gaps: the antiferromagnetic order coupled to the sublattice and a spin-valley coupling, being responsible for time symmetry and inversion breaking, respectively [46, 47]. The situation corresponds exactly to the masses represented in Eq. (11). However, the spin remains degenerate due to the antiferromagnetic (AFM) coupling between two inequivalent Mn ions.

In order to generate the necessary split between the spin bands, two types of setups can be prepared. One of them consists of doping the material, replacing for example one Mn atom by a Zn atom. The imbalance in spin will generate a magnetization, and consequently a spin splitting in the bands, while still retaining the different valleys [48]. This procedure results in a band structure schematically represented in Fig. 1(e). Another possible way is to use an heterojunction of different 2D materials such as MnPSe<sub>3</sub>/CrBr<sub>3</sub> [49], MnPSe<sub>3</sub>/MoS<sub>2</sub> [50] and WS<sub>2</sub>/h-VN [51].

Besides the aforementioned heterostructures, dichalcogenides like NbSe<sub>2</sub> and WS<sub>2</sub> also seem promising to simultaneously lift both valley and spin degeneracy. This can be either reached by using a substrate [53] to WS<sub>2</sub>, or as by using a 2D magnetic semiconductor as monolayer NbSe<sub>2</sub> with its large valley-polarized state [54]. In such system, no external influence by either doping, substrating or van der Waals couplings is necessary, rather the magnetic state is sufficient to completely split the bands, resulting in the generation of a valley-polarized state with a spontaneously occurring valley current [55, 56].

#### IV. CONCLUSION

We proposed a robust analog of the CME in condensed matter, which can be realized in two-dimensional materials. As its raison d'être is the parity rather than chiral anomaly, we may call it the parity magnetic effect.

Besides, we showed that this analog is intimately related to an intrinsic half-integer anomalous Quantum Hall effect<sup>1</sup>. We offered several setups that follow the criteria to source this mechanism. Our 2D PME proposal offers remarkable benefits compared to the 3D materials where the chiral magnetic effect has been performed so far. First of all, the pseudo-chiral imbalance is intrinsic in the structures, while three-dimensional Dirac materials like  $ZrTe_5$  necessarily need external fields to activate it. Besides that, chiral fermions in three-dimensional Dirac/Weyl semimetals generally undergo chirality-changing scattering. This induces a reduction in the intensity of a DC current, the latter being subject to a characteristic relaxation time  $\tau$ . The setups we propose are free from that, since the currents are topologically protected. Therefore, we expect that our findings may open a new window to explore magnetic field driven current in planar materials, significantly simplifying the setup and offering potential advantages in the search for new anomalous transport phenomena.

#### ACKNOWLEDGMENTS

A. J.M. receives partial support from FAPESP under fellowship number 2016/12705-7. F. M. thanks CNPq, Grant No. 381511/2018-9 and FAPESP, grant No. 2020/06896-0 for financial support. C. V. acknowledges financial support from FONDECYT under grants 1190192 and 1200483. We thank A. Saraiva, I. Shovkovy, S. Mellaerts and M. Houssa for fruitful discussions.

### Appendix A: The fermion mass sector in two-component spinor language

The mass terms appearing in Eq. (5) of the main body of our paper are written in four-component spinor language in the pseudo-chiral basis, meaning that<sup>2</sup>

$$\psi_{\chi} = \begin{pmatrix} \psi_{+} \\ 0 \end{pmatrix}, \qquad \psi_{\chi'} = \begin{pmatrix} 0 \\ \psi_{-} \end{pmatrix}$$
(A1)

using two two-component spinors  $\psi_{\pm}$ . Since

$$\gamma_0 = \begin{pmatrix} 0 & \mathbb{1}_2 \\ \mathbb{1}_2 & 0 \end{pmatrix}, \qquad \gamma_z = \begin{pmatrix} 0 & \sigma_z \\ -\sigma_z & 0 \end{pmatrix},$$
(A2)

the mass terms  $(m_{\chi} > 0, m_{\chi'} > 0)$ 

$$S_{\text{mass}} = \int d^3x \left( \bar{\psi}_{\chi} (\mu \gamma_0 + m_{\chi} \gamma_z) \psi_{\chi} + \bar{\psi}_{\chi'} (\mu \gamma_0 + m_{\chi'} \gamma_z) \psi_{\chi'} \right)$$
 (A3)

can be rewritten as

$$S_{\text{mass}} = \int d^3x \left( \bar{\psi}_+ (\mu \sigma_z - m_\chi) \psi_+ + \bar{\psi}_- (\mu \sigma_z + m_{\chi'}) \psi_- \right), \tag{A4}$$

keeping in mind that in (2+1)-dimensions,  $\sigma_z$  plays the role of  $\gamma_0$  in an appropriate basis [57].

This shows that we actually have two two-components spinors with opposite sign standard masses. This plays a pivotal role in our analysis.

#### Appendix B: Linear response theory applied to Reduced Quantum Electrodynamics

Linear response theory investigates the reaction of a system under a small external influence assuming that this reaction can be studied at linear order in the external stimulus. Here we apply this procedure to calculate the conductivity of the continuum quantum field theory description of a material sample organized in a (2+1)-dimensional honeycomb lattice when a constant external magnetic field is applied in-plane.

 $<sup>^1</sup>$  Interestingly, for another class of transition metal chalcogenides, like  $\rm V_2O_3$ , recent computations of [65, 66] suggest that the two valleys contribute with equal sign mass to the dynamical Chern-Simons term, something which should be related to the strong spin-orbit coupling. This could lead to an intrinsic integer rather than half-integer PME conductivity. This deserves further scrutiny in the future.  $^2$  We suppress the spin index s for now.

A certain care is needed since this is a mixed-dimensional theory: the charge carriers are constrained to a plane while the gauge fields live in a bulk. The theory to describe such systems has been developed previously and is known as pseudo-Quantum Electrodynamics (PQED) [35, 36] or reduced-Quantum Electrodynamics (RQED) [37]. Here we present in detail how to introduce the interaction with the external magnetic field. In this Appendix, for the sake of clarity, we refer to the dimension of the system using the usual quantum field theory notation (n-space +1-time)-dimension, in contradistinction with the condensed matter conventional notation used in the main body of the manuscript.

We use the external field configuration as set out in Eqs. (6)-(8), where the DC limit  $\omega \to 0$  is understood. The classical action in (3+1)-dimensions is given by

$$S = \frac{1}{4} \int d^4x F_{\mu\nu}^2 + \int d^3x \bar{\psi}(\vec{x}, 0) i \not D\psi(\vec{x}, 0) + \text{fermion mass terms} + \text{gauge fixing}, \tag{B1}$$

where the vector  $\vec{x} = (t, x, y)$  and the covariant derivative  $\not D = (\partial_0 + ieA_0)\gamma_0 + v_F(\partial_x + ieA_x)\gamma_x + v_F(\partial_y + ieA_y)\gamma_y$ , since the (fermion) electronic degrees of freedom propagate on the z = 0 surface.

One can check the full gauge invariance of the (3 + 1)-dimensional action in Eq. (B1), applying

$$\psi(\vec{x},0) \to e^{ie\alpha(x)}\psi(\vec{x},0), \quad \bar{\psi}(\vec{x},0) \to e^{-ie\alpha(x)}\bar{\psi}(\vec{x},0), \quad A_{\mu}(x) \to A_{\mu}(x) - \partial_{\mu}\alpha(x),$$

with 4-vector  $x = (\vec{x}, z)$ .

The Noether current is easily identified as

$$j_{\mu}(\vec{x}) = \bar{\psi}(\vec{x}, 0)\gamma_{\mu}\psi(\vec{x}, 0). \tag{B2}$$

This current is gauge invariant and conserved on-shell, as expected. It is also independent from the z-coordinate. The third component  $j_z$  can be written down formally, but it does not correspond to the transport of any physical electric charge, as can be easily checked using the integrated Gauss' law. So effectively,  $j_z = 0$ .

We notice that  $j_{\mu}$  has mass dimension 2, as corresponding to a (2+1)-dimensional current. Let us introduce its (3+1)-dimensional version,

$$J_{\mu}(x) = j_{\mu}(\vec{x})\delta(z) \tag{B3}$$

to properly disturb the action S with

$$\int d^4x J_{\mu}(x) a_{\mu}(x) = \int d^4x j_y(\vec{x}) \frac{iB}{\omega} \cos(\omega t) e^{i\omega z} \delta(z) = \int d^3x j_y(\vec{x}) \frac{iB}{\omega} \cos(\omega t)$$

to set up the appropriate Kubo linear response theory.

The (still mixed-dimensional) perturbed action can thus be written as

$$\widetilde{S} = \frac{1}{4} \int d^4x F_{\mu\nu}^2 + \int d^3x \bar{\psi}(\vec{x}, 0) (i\not\!D) \psi(\vec{x}, 0) + \int d^4x J_{\mu}(x) a_{\mu}(x)$$
+ fermion masses + gauge fixing. (B4)

Following e.g. [58] and transforming to momentum (Fourier) space, it can be shown that the action in Eq. (B4) can be reduced to an equivalent, be it purely (2+1)-dimensional, action

$$\widetilde{S} = \frac{1}{2} \int d^3x F_{\mu\nu} \frac{1}{\sqrt{-\partial^2}} F_{\mu\nu} + \int d^3x \bar{\psi} i \not \!\! D \psi + \int d^3x j_y(\vec{x}) \left( \frac{iB}{\omega} \cos(\omega t) \right)$$
+ fermion masses + gauge fixing. (B5)

We recognize here RQED, supplemented with an external disturbance. Doing so, we can now depart from this consistent (2+1)-dimensional action to extract the DC conductivity via a Kubo relation. There is no more reference to the obsolete z-direction. This also makes clear why we chose the vector potential (7), which is by no means unique, along the  $\vec{e_y}$ -direction, as this choice allows a full dimensional reduction of the relevant dynamics.

Closely following [40], we have a disturbed Hamiltonian given by  $\Delta H = -\vec{j} \cdot \vec{a}$ , from now on always assuming z = 0. The expectation value of the current to leading order in  $\vec{a}$  becomes

$$\langle \vec{j}(t) \rangle = \frac{i}{\hbar} \langle 0 | \int_{-\infty}^{t} d\tau [\Delta H(\tau), \vec{j}(t)] | 0 \rangle.$$
 (B6)

or concretely, given that the commutator of the Hermitian currents is purely imaginery,

$$\langle j_x(t) \rangle = \frac{iB}{\hbar\omega} \langle 0 | i \int_{-\infty}^{t} d\tau [j_y(\tau), j_x(t)] | 0 \rangle \cos(\omega\tau) = \operatorname{Im} \left\{ \frac{B}{\hbar\omega} \langle 0 | i \int_{-\infty}^{t} d\tau [j_y(\tau), j_x(t)] | 0 \rangle e^{-i\omega\tau} \right\}.$$
 (B7)

Then, after using time translational invariance, we get

$$\langle j_x(t) \rangle = \frac{B}{\hbar \omega} \operatorname{Im} \left\{ i \int_0^\infty d\tau \left( \langle 0 | [j_y(0), j_x(\tau)] | 0 \rangle e^{i\omega\tau} \right) e^{-i\omega t} \right\}, \tag{B8}$$

from which the Kubo relation for the DC PME anomalous conductivity follows as

$$\sigma = \lim_{\omega \to 0} \frac{1}{\hbar \omega} \operatorname{Im} \left\{ i \int_0^\infty d\tau e^{i\omega\tau} \left\langle 0 | \left[ j_y(0), j_x(\tau) \right] | 0 \right\rangle \right\}. \tag{B9}$$

We stress here again that we are looking at a current induced by and parallel to a magnetic field.

As we are interested in the  $\omega \to 0$  limit, it will be sufficient to evaluate the integral in Eq. (B9) up to  $\mathcal{O}(\omega)$ . As the integrand in the r.h.s. of Eq. (B9) is actually the retarded correlator, we can use the fact that retarded and Euclidean correlator coincide at  $\omega = 0$  [62], an identification valid since the Euclidean photon self-energy  $\Pi^{ij}$  has no pole at zero frequency, see Eq. (B10).

Assuming as before a standard Dirac mass m for the two-component spinor and a chemical potential  $\mu$ , it can be shown that the low-energy limit of the induced T-odd part in the RQED photon self-energy is one-loop exact [38], a generalization of the Coleman-Hill theorem [39]. This leads to a Chern-Simons term in the photon effective action. More precisely, the (transverse and gauge invariant) photon self-energy—which corresponds to the current-current correlator and as such is equivalent to its (2+1)-dimensional QED counterpart at one-loop—reads in Euclidean space (with  $p_0 = \omega$ )

$$\tilde{\Pi}^{ij}(\vec{p}) = -\frac{m}{|m|} \frac{e^2}{4\pi} \theta(m^2 - \mu^2) \epsilon^{ijk} p_k + \mathcal{O}(p^2), \tag{B10}$$

see e.g. [59–61] for several ways to compute. There is actually no ambiguity in the leading infrared behaviour of  $\tilde{\Pi}^{ij}(\vec{p})$ . Indeed, the very same coefficient is found when the limits are taken as  $p_0 = 0$ ,  $\vec{p} \to 0$ , see [33, 34].

As such, we get from Eqs. (B9), (B10) that

$$\sigma = -\lim_{\omega \to 0} \frac{1}{\hbar \omega} \Pi^{yx} = \lim_{\omega \to 0} \frac{1}{\hbar \omega} \frac{m}{|m|} \frac{e^2}{4\pi} \theta(m^2 - \mu^2) \epsilon_{210} \omega = -\frac{e^2}{4\pi \hbar} \frac{m}{|m|} \theta(m^2 - \mu^2).$$
 (B11)

This DC conductivity will receive no further corrections, given the one-loop exactness of  $\Pi^{yx}(\omega)$  for vanishing frequency. This is suggestive of the fact the conductivity might have a topological origin, something that will be discussed further in the next Section.

This result for  $\sigma$  is the expression we relied on in the main body of the text to derive our final expression for the anomalous conductivity, in the case that only a single spin-band contributes, with 2 different two-component spinors (one per Dirac point) with masses  $m_{\chi} > 0$  and  $-m_{\chi'} < 0$ ,

$$\sigma_{\chi} = \frac{e^2}{4\pi\hbar} \left( \frac{m_{\chi}}{|m_{\chi}|} \theta(m_{\chi}^2 - \mu^2) - \frac{m_{\chi'}}{|m_{\chi'}|} \theta(m_{\chi'}^2 - \mu^2) \right).$$
 (B12)

Assuming as in the main body of our paper that  $m_{\chi'}^2 < \mu^2 < m_{\chi}^2$ , the predicted value for the conductivity becomes

$$\sigma_{\chi} = \frac{e^2}{2h},\tag{B13}$$

which corresponds to a *half-integer* anomalous quantum Hall conductivity capable of sustaining a current along an externally applied magnetic field.

# Appendix C: Half-integer topology of the anomalous conductivity

Reconsidering Eq. (B9), and using the undisturbed energy eigenbasis,  $|n\rangle$ , and Hamiltonian time evolution with initial time t=0,  $\vec{j}(t)=e^{i\frac{H_0t}{\hbar}}\vec{j}e^{-i\frac{H_0t}{\hbar}}$ , we may rewrite it as

$$\sigma = -\lim_{\omega \to 0} \frac{1}{\hbar \omega} \int_0^\infty d\tau e^{i\omega\tau} \sum_n \left( \langle 0|j_y|n\rangle \langle n|j_x|0\rangle e^{\frac{i}{\hbar}(E_n - E_0)t} - \langle 0|j_x|n\rangle \langle n|j_y|0\rangle e^{\frac{i}{\hbar}(E_0 - E_n)t} \right). \tag{C1}$$

Integrating over  $\tau$  and expanding to leading order in  $\omega$  again, we arrive at

$$\sigma = 2\hbar \operatorname{Im} \sum_{n \neq 0} \frac{\langle 0|j_y|n\rangle \langle n|j_x|0\rangle}{(E_n - E_0)^2}.$$
 (C2)

No divergence in  $\frac{1}{\omega}$  hampers the discussion as the photon self-energy (viz. current correlator) starts at  $\mathcal{O}(\omega)$ , see [38] for an explicit proof based on a Ward identity (in se gauge invariance).

Proceeding as in [40] by introducing for both  $\alpha$  filled bands and  $\beta$  unfilled bands the Bloch wave functions,  $\Psi_{\vec{p}}^{\alpha,\beta}(\vec{x}) = e^{i\vec{p}\cdot\vec{x}}u_{\vec{n}}^{\alpha,\beta}(\vec{x})$ , we can rewrite Eq. (C2) using a compact notation

$$\sigma = 2\hbar \operatorname{Im} \sum_{E_{\alpha} < \mu < E_{\beta}} \int_{T^2} \frac{d^2 p}{(2\pi)^2} \frac{\langle u_{\vec{p}}^{\alpha} | j_y | u_{\vec{p}}^{\beta} \rangle \langle u_{\vec{p}}^{\beta} | j_x | u_{\vec{p}}^{\alpha} \rangle}{(E_{\beta} - E_{\alpha})^2}, \tag{C3}$$

where the 2-dimensional  $\vec{p}$  lives on the Brillouin zone  $T^2$ . This expression can be further massaged into

$$\sigma = \frac{2e^2}{\hbar} \operatorname{Im} \sum_{\alpha} \int_{T^2} \frac{d^2 p}{(2\pi)^2} \left\langle \partial_{p_y} u_{\vec{p}}^{\alpha} | \partial_{p_x} u_{\vec{p}}^{\alpha} \right\rangle = \frac{e^2}{\hbar} \sum_{\alpha} C_{\alpha}$$
 (C4)

once the current in Fourier space is identified as  $\vec{j} = \frac{e}{\hbar} \nabla_{\vec{p}} \widetilde{H}$ , with  $\widetilde{H} = e^{-i\vec{p}\cdot\vec{x}} H e^{i\vec{p}\cdot\vec{x}}$ , the Hamiltonian with momentum shifted over  $\hbar \vec{p}$ . To arrive at Eq. (C4), it was tacitly assumed that the bands are gap-separated, with chemical potential  $\mu$  in such gap. The final outcome is the well-known sum over the integer Chern numbers  $\mathcal{C}_{\alpha}$  per filled band [64], thereby disposing the topological character of the conductivity.

However, we should be careful when applying Eq. (C4) directly to our case, as one of the underlying conditions is not met. Indeed, a crux of our setup is that the chemical potential  $\mu$  was chosen in the gap between the 2 Dirac points. Evidently, this leads to a "cutting" of the respective band, see Fig. 1(d) in the main body of our paper. Let us therefore analyze the expression (C6) a bit better in the case the underlying low energy effective Hamiltonian per valley per spin is of the type<sup>3</sup> [63]

$$H(\vec{p}) = h_0(\vec{p})\mathbb{1}_2 + h_i(\vec{p})\sigma_i. \tag{C5}$$

Then, using the "ray method", it was shown in [63] that the Chern number receives a contribution  $\pm \frac{1}{2}$  per massive Dirac point (cone). If the full band is taken into account for a double cone system (as we have), this will automatically lead to an integer Chern number and thence  $\sigma = \pm \frac{e^2}{h}$ , 0 as possible conductivities.

However, due to our judicious choice of  $\mu$  in the finite intervalley gap between the K and K' Dirac points, we are

However, due to our judicious choice of  $\mu$  in the finite intervalley gap between the K and K' Dirac points, we are effectively cutting away part of that band and only a single cone will contribute to the conductivity. Denoting with  $\alpha'$  all completely filled bands and singling out that "partially cut" band (the encircled piece), we actually have

$$\sigma_{\chi} = \frac{e^2}{h} \sum_{\alpha'} C_{\alpha'} \pm \underbrace{\left(\frac{e^2}{h} \frac{1}{2}\right)}_{\text{integer}},\tag{C6}$$

where the encircled piece is only there for the spin projection that is partially filled, the sign in front depending on which of the 2 Dirac points is the contributing one. Remember also that we lifted the spin degeneracy to avoid a net cancellation of the current; the other spin projection band is thus not filled and as such not contributing. This encircled piece exactly confirms the result (B13) found before using an explicit quantum field theory computation and as promised, despite its half-integer character, the above reasoning shows it still carries a topological meaning. Indeed, small perturbations will preserve the fact that only a single Dirac point contributes, which always happens with a value of  $\pm \frac{1}{2}$ .

<sup>[1]</sup> Kharzeev, D. E., McLerran, L. D. & Warringa, H. J. The Effects of topological charge change in heavy ion collisions: 'Event by event P and CP violation'. Nucl. Phys. A 803, 227 (2008).

<sup>&</sup>lt;sup>3</sup> The few materials that we already identified in our main body of the text with the desired gap structure are all of this type. To be more precise, they are of the graphene-type, but supplemented with a specific mass term along the  $\sigma^z$ -direction.

- [2] Fukushima, K., Kharzeev, D. E. & Warringa, H. J. The Chiral Magnetic Effect. Phys. Rev. D 78, 074033 (2008).
- [3] Koch, V. et al. Status of the chiral magnetic effect and collisions of isobars. Chin. Phys. C 41, no. 7, 072001 (2017).
- [4] Zhao, J. & Wang, F. Experimental searches for the chiral magnetic effect in heavy-ion collisions. Prog. Part. Nucl. Phys. **107**, 200-236 (2019).
- [5] Novoselov, K. S. et al. Two-dimensional gas of massless Dirac fermions in graphene. Nature 438, 197–200 (2005).
- [6] Katsnelson, M., Novoselov, K. & Geim, A. Chiral tunnelling and the Klein paradox in graphene. Nature Physics 2, 620–625 (2006).
- [7] Katsnelson, M. Zitterbewegung, chirality, and minimal conductivity in graphene. Eur. Phys. J. B 51, 157–160 (2006).
- [8] Li, Q. et al. Chiral magnetic effect in ZrTe5. Nature Phys. 12, 550 (2016).
- [9] Geim, A., Novoselov, K. The rise of graphene. Nature Mater 6, 183 (2007).
- [10] P. Miró, M. Audiffreda and T. Heine, An atlas of two-dimensional materials. Chem. Soc. Rev., 6537, 43, (2014).
- [11] A.K. Geim and I.V. Grigorieva, Van der Waals heterostructures, Nature, 499, 419 (2013).
- [12] Zheng, G. et al. Transport evidence for the three-dimensional Dirac semimetal phase in ZrTe5. Phys. Rev. B 93, 115414 (2016).
- [13] Li, C. et al. Giant negative magnetoresistance induced by the chiral anomaly in individual Cd3As2 nanowires. Nature Communications 6, 10137 (2015).
- [14] Huang, X. et al. Observation of the Chiral-Anomaly-Induced Negative Magnetoresistance in 3D Weyl Semimetal TaAs. Phys. Rev. X 5, 031023 (2015).
- [15] Z. Wang et al. Helicity-protected ultrahigh mobility Weyl fermions in NbP. Phys. Rev. B 93, 121112 (2016).
- [16] Arnold, F. et al. Nature Communications 7, 11615 (2016).
- [17] Zhang, C. et al. Room-temperature chiral charge pumping in Dirac semimetals. Nature Communications 8, 13741 (2017).
- [18] Nielsen, H. B. & Ninomiya, M. Adler-Bell-Jackiw anomaly and Weyl fermions in a crystal. Phys. Lett. B 130, 389-396 (1983).
- [19] Gusynin, V. P., Sharapov, S. G. & Carbotte, J. P. AC conductivity of graphene: from tight-binding model to 2+1-dimensional quantum electrodynamics. Int. J. Mod. Phys. B 21, 4611-4658 (2007).
- [20] Katsnelson, M. I. Graphene: Carbon In Two Dimensions, Cambridge University Press, New York (2012).
- [21] Galicia, M. J. A. and Bashir, A. Fermions in odd space-time dimensions: Back to basics. Few Body Syst. 37, 71-78 (2005).
- [22] Castro-Neto, A. H., Guinea, F., Peres, N. M. R., Novoselov, K. S., Geim, A. K. The electronic properties of graphene. Rev. Mod. Phys. 81, 109 (2009).
- [23] Song, D. et al, Unveiling pseudospin and angular momentum in photonic graphene. Nature Communications 6, 6272 (2015).
- [24] Mecklenburg, M. & Regan, C. B. Spin and the Honeycomb Lattice: Lessons from Graphene. Phys. Rev. Lett. 106, 116803 (2011).
- [25] Redlich, A.N., Gauge Noninvariance and Parity Violation of Three-Dimensional Fermions, Phys. Rev. Lett. 52, 18 (1984).
- [26] Semenoff, G. W. Condensed-Matter Simulation of a Three-Dimensional Anomaly. Phys. Rev. Lett. 53, 2449 (1984).
- [27] Niemi, A. J. & Semenoff, G. W. Axial Anomaly Induced Fermion Fractionization and Effective Gauge Theory Actions in Odd Dimensional Space-Times. Phys. Rev. Lett. **51**, 2077 (1983).
- [28] Poppitz, E. R. Induced Chern-Simons terms at finite temperature. Phys. Lett. B 252, 417-419 (1990).
- [29] Mizher, A. J., Raya, A. & Villavicencio, C. Electric current generation in distorted graphene. Int. J. Mod. Phys. B 30, no. 2, 1550257 (2015).
- [30] Mizher, A. J., Hernandez-Ortiz, S. , Raya, A. & Villavicencio, C. Aspects of the pseudo Chiral Magnetic Effect in 2D Weyl-Dirac Matter. Eur. Phys. J. C 78, no. 11, 912 (2018).
- [31] Thouless, D. J., Kohmoto, M., Nightingale, M. P. & den Nijs, M. Quantized Hall Conductance in a Two-Dimensional Periodic Potential. Phys. Rev. Lett. 49, 405 (1982).
- [32] Marino, E. C., Nascimento, L. O., Alves, V. S. & Smith, C. M. Interaction Induced Quantum Valley Hall Effect in Graphene. Phys. Rev. X 5, 011040 (2015).
- [33] Zeitlin, V. Comment on 'Dynamical Chern-Simons term generation at finite density' and 'Chern-Simons term at finite density', [arXiv:hep-th/9612225 [hep-th]];
- [34] Zeitlin, V. Induced magnetic field in a finite fermion density Maxwell QED in (2+1)-dimensions," Mod. Phys. Lett. A 12, 877-886 (1997).
- [35] Marino, E. Quantum electrodynamics of particles on a plane and the Chern-Simons theory. Nucl. Phys. B 408, 551 (1993).
- [36] Nascimento, L, O., Alves, V. S., Peña, F., Smith, C. M. & Marino, E. C. Chiral-symmetry breaking in pseudoquantum electrodynamics at finite temperature. Phys. Rev. D **92**, 025018 (2015).
- [37] Gorbar, E. V., Gusynin, V. P. & Miransky, V. A. Dynamical chiral symmetry breaking on a brane in reduced QED. Phys. Rev. D 64, 105028 (2001).
- [38] Dudal, D., Mizher, A. J. & Pais, P. Remarks on the Chern-Simons photon term in the QED description of graphene. Phys. Rev. D **98**, no. 6, 065008 (2018).
- [39] Coleman, S. R. & Hill, B. R. No More Corrections to the Topological Mass Term in QED in Three-Dimensions. Phys. Lett. B 159, 184-188 (1985).
- [40] Tong, D. Lectures on the Quantum Hall Effect, given at the Tata Institute of Fundamental Research, Mumbai (2016) [arXiv:1606.06687 [hep-th]].
- [41] Liu, C.-X., Zhang, S.-C. & Qi, X.-L. The quantum anomalous Hall effect: theory and experiment. Ann. Rev. Cond. Mat. Phys. 7, 301-321 (2016).
- [42] Haldane, F. D. M. Model for a Quantum Hall Effect without Landau Levels: Condensed-Matter Realization of the 'Parity Anomaly'. Phys. Rev. Lett. **61**, 2015-2018 (1988).

- [43] Kharzeev, D. E. & Warringa, H. J. Chiral Magnetic conductivity. Phys. Rev. D 80, 034028 (2009).
- [44] Kane, C. L. & Mele, E. J. Quantum Spin Hall Effect in Graphene. Phys. Rev. Lett. 95, 226801 (2005).
- [45] Meng, Z. Y., Lang, T. C., Wessel, S., Assaad, F. F. & Muramatsu, A. Quantum spin liquid emerging in two-dimensional correlated Dirac fermions. Nature 464, 847–851 (2010).
- [46] Li, X., Wu, X. & Yang, J. Half-Metallicity in MnPSe3 Exfoliated Nanosheet with Carrier Doping. J. Am. Chem. Soc. 136 31, 11065–11069 (2014).
- [47] Li, X., Cao, T., Niu, Q., Shi, J. & Feng, J. Coupling the valley degree of freedom to antiferromagnetic order. PNAS 110 (10) 3738-3742 (2013).
- [48] Zhong, L., Chen, X. & Qi, J. Controlling the spin and valley degeneracy splitting in monolayer MnPSe3 by atom doping. Phys. Chem. Chem. Phys. 19, 15388-15393 (2017).
- [49] Wun, X. Modulation of spin-valley splitting in a twodimensional MnPSe3/CrBr3 van der Waals heterostructure. J. Phys. D: Appl. Phys. **53**, 125104 (2020).
- [50] Pei, Q., Song, Y., Wang, X., Zou, J. & Mi, W., Superior Electronic Structure in Two-Dimensional MnPSe3 /MoS2 van der Waals Heterostructures. Scientific Reports 7, 9504 (2017).
- [51] Ke, C. et al. Large and controllable spin-valley splitting in two-dimensional WS2/h-VN heterostructure. Phys. Rev. B 100, 195435 (2019).
- [52] Wiedenmann, A., Rossat-Mignod, J., Louisy, A., Brec, R. & Rouxel, J. Neutron diffraction study of the layered compounds MnPSe3 and FePSe3. Solid State Communication, 40, 1067 (1981).
- [53] Norden, T. et al. Giant valley splitting in monolayer WS2 by magnetic proximity effect. Nature Communications 10, 4163 (2019).
- [54] Zang, Y. et al. Large valley-polarized state in single-layer NbX2 (X = S, Se): Theoretical prediction. Nano Research 14, 834-839 (2021).
- [55] Xiao, D., Yao, W. & Niu, Q. Valley-Contrasting Physics in Graphene: Magnetic Moment and Topological Transport. Phys. Rev. Lett. 99, 236809 (2007).
- [56] Li, S. et al. Valley-dependent properties of monolayer MoSi2N4, WSi2N4 and MoSi2As4. Phys. Rev. B 77, 235406 (2008).
- [57] Dunne, G. V. Aspects of Chern-Simons theory, lectures given at the 1998 Les Houches Summer School: Topological Aspects of Low Dimensional Systems [arXiv:hep-th/9902115 [hep-th]].
- [58] Dudal, D., Mizher, A. J. & Pais P. Exact quantum scale invariance of three-dimensional reduced QED theories, Phys. Rev. D 99, no.4, 045017 (2019).
- [59] Niemi, A. J. & Semenoff, G. W. Fermion Number Fractionization in Quantum Field Theory, Phys. Rept. 135, 99 (1986).
- [60] Poppitz, E. R. Induced Chern-Simons terms at finite temperature, Phys. Lett. B 252, 417-419 (1990).
- [61] Sisakian, A. N., Shevchenko, O. Y. & Solganik, S. B. Chern-Simons term at finite density, Phys. Lett. B 403, 75-79 (1997).
- [62] Meyer, H. B. The Bulk Channel in Thermal Gauge Theories, JHEP 04, 099 (2010).
- [63] Sticlet, D., Piéchon, F., Fuchs, J.-N., Kalugin. P. & Simon, P. Geometrical engineering of a two-band Chern insulator in two dimensions with arbitrary topological index, Phys. Rev. B 85, 165456 (2012).
- [64] Thouless, D. J., Kohmoto, M. Nightingale, M. P. & den Nijs, M. Quantized Hall Conductance in a Two-Dimensional Periodic Potential, Phys. Rev. Lett. 49, 405-408 (1982).
- [65] Mellaerts, S., Meng. R., Menghini. M, Afanasiev. V, Seo J.W., Houssa. M. & Loquet, J.-P. Two-dimensional honeycombkagome V2O3: a robust room-temperature magnetic Chern insulator interfaced with graphene, [arXiv:2101.02162 [condmat.mes-hall]].
- [66] Mellaerts, S., Meng, R., Afanasiev, V., Seo, J.W, Houssa, M. & Locquet, J.-P. Quarter-filled Kane-Mele Hubbard model: Dirac half-metals, Phys. Rev. B 103, 155159 (2021).